Exploring Blood Flow Dynamics Underlying Pathogenesis of Splenic Artery Aneurysms

Kirsten B. Giesbrecht[*1]
Advisor: Dr. Ellen R. Swanson [†1]

[1]Centre College, Department of Mathematics;

Abstract

If an expectant mother develops a splenic artery aneurysm that ruptures, there is a 90% fetal mortality rate. Splenic artery aneurysms account for 46-60% of visceral aneurysms in the human abdomen. The cause for the propensity of aneurysms to develop and rupture along the splenic artery is unknown. A distinguishing characteristic of this artery is its tortuous shape. We investigate how the unique geometries of the artery may lead to unusual patterns in blood flow. Dramatic changes in blood flow properties such as blood pressure, velocity and wall shear are conducive for aneurysm formation, development, and rupture. Using Ansys Fluent computational fluid dynamics software, the influence of these elements of blood flow through both straight and curved arteries is explored. Under identical initial and boundary conditions, the curved artery reaches both higher dynamic pressure and wall shear stress values than the straight artery. The curved artery also has a greater range of dynamic pressure and wall shear stress values compared to the range of values in the straight artery. Additionally, blood flow changes associated with pregnancy, including increased peak velocity, are shown to increase the risk of aneurysm development and rupture. These results indicate that the curved geometry of the splenic artery predisposes it to promote aneurysm rupture and growth.

1 Introduction

Aneurysms are a localized widening or bulging of a blood vessel due to weakening arterial walls. Aneurysms may be either fusiform or saccular in shape. Fusiform aneurysms are characterized by the diameter of the artery increasing uniformly throughout the aneurysm location and have no neck extruding from the artery. A saccular aneurysm has a localized bulging in the artery on one side and has a neck protruding from the artery. In humans, aneurysms are most commonly found in the brain and aorta [24]. While the cause of aneurysms is unknown, atherosclerosis and high blood pressure are associated with increasing risks for developing aneurysms [24]. The rupture of an aneurysm may lead to internal bleeding, strokes, and possibly death [22].

The splenic artery carries blood from the celiac trunk, a branch of arteries on the aorta, to the spleen, along a tortuous and undulating path. This curving shape distinguishes the artery from all the other relatively straight arteries in the body [17]. The splenic artery is located on the left side of the torso, across from the liver and above the stomach and left kidney.

In addition to its strange shape, the splenic artery is also the most common site for aneurysms to develop in splanchnic arteries [23, 17, 16]. Splanchnic arteries include all arteries in the body cavity excluding the aorta. The splenic artery accounts for 46-60 % of these visceral aneurysms [16, 7, 18]. Typically, splenic artery aneurysms (SAAs) are saccular and form in groups of two to three aneurysms along the splenic artery. Surgery is usually recommended when an aneurysm reaches 2 cm in diameter [7]. Approximately 10-36% of ruptured splenic artery aneurysms are fatal [23, 16].

Taking preventative measures against ruptured splenic artery aneurysms is difficult since SAAs are often asymptomatic. Only 5% of patients develop symptoms prior to the artery rupturing [23]. Often unruptured SAAs are

---

[*]kirs10gies@gmail.com
[†]ellen.swanson@centre.edu

discovered during medical imaging for patients with other visceral diseases [7]. Other times SAAs are discovered post-mortemly during autopsies.

Accurately measuring how much of the population may be affected by SAAs is difficult due to their asymptomatic nature, but it is estimated that SAAs affect 0.01-10% of the population [23]. SAAs also disproportionately affect women more than men. Most abdominal artery aneurysms are equally common in men as they are in women [23, 16], however SAAs are four times more commonly found in women than they are in men [23]. Women who have had multiple pregnancies [16, 23], patients who have had a splenomegaly, or patients who have had an orthotropic liver transplantation within the past year are at an increased risk for developing a SAA [16, 11]. Women who have been pregnant or who are currently pregnant are at the highest risk of developing a SAA [23, 18].

Approximately a quarter of all reported SAAs occur in pregnant women [23] and half of ruptured SAAs occur in women who are pregnant or who had been pregnant previously [18]. Although the rupture of the splenic artery is relatively rare, the mortality rate of a ruptured splenic artery is especially high in pregnant women. The fetal mortality rate is 90%; while the mortality rate of the mother is 70% [18].

Pregnant women undergo several blood flow changes throughout a pregnancy. Peak blood velocity increases as a result of an increased volume of blood that flows through the body during the pregnancy [21]. This change in velocity may affect other hemodynamic variables that underlie aneurysm pathogenesis and rupture such as pressure.

The splenic artery is characterized by two unique properties; its undulating shape and its popularity as a site for visceral aneurysm development and rupture. While risks associated with developing SAAs have been identified, the mechanism for the high prevalence of aneurysms in the splenic artery compared to other abdominal arteries is still unknown. Previous studies have not investigated how the unique shape of the artery may influence aneurysm development.

Simulation of blood flow within the artery using numerical methods is a well established and reliable technique for studying the physiological underpinnings of aneurysms [20, 6]. Gonzalez et al. [6] show that computational fluid dynamics modeling is an attractive method for examining aneurysms since the simulations will not disrupt the hemodynamic environment of the artery and aneurysm. In vivo methods for measuring blood flow may influence the system [6]. When medical devices are used to measure hemodynamic conditions, they pose the risk of disturbing the delicate hemodynamic environment within the artery. Additionally, it can be difficult to measure the hemodynamic factors in vivo [20]. In addition to being a non-invasive method, computational fluid dynamics has also been shown to be an accurate method for studying artery hemodynamics. Steinman et al. [20] use rigid patient specific geometries to study blood flow in CFD simulations of cerebral aneurysms. They found results obtained from their rigid CFD model to be consistent with those obtained from in vivo measurements of blood flow using contrast injected into arteries. Using rigid arteries to model aneurysms is common in computational fluid dynamics models and is often employed to compare how geometric differences within aneurysms and arteries may influence hemodynamics of the aneurysm [5, 19, 2, 20]. Shishir et al. [19] vary geometric factors such as aneurysm neck size and shape in rigid arteries to compare hemodynamic factors including pressure, wall shear stress, and vortices within aneurysms of rigid arteries [19]. Hoi et al. [8] examine degrees of curvature in similar CFD simulations [8]. We use CFD simulations and create a generalized model of a splenic artery that is not patient specific. We use the finite volume method to simulate the blood flow and the Ansys Fluent software package to solve for the equations describing fluid flow. The finite volume method is less dependent on the quality of the meshes than the finite element method in producing the same results [9].

We propose that the splenic artery is such a common site for aneurysms in visceral arteries due to its tortuous geometry which predisposes it for aneurysm development and for aneurysm growth and rupture. Examining how geometry may impact hemodynamics and aneurysm pathogenesis has been previously studied in cerebral aneurysms [8]. Using three-dimensional CFD simulations, Hoi et al. [8] conclude that hemodynamic stresses, such as wall shear stress, increased as the arterial curvature increased. However, similar studies examining geometric properties have not been conducted for splenic arteries. Additionally, we propose that increased blood velocity characteristic of pregnancy exacerbates these conditions. We describe the mathematical model used in §2.1. We construct artery geometries of a splenic artery and a straight artery in §2.2 to investigate how the geometry affects blood flow. We examine blood flow factors in §2.3 and set boundary conditions in §2.4. In §3.1, we examine blood flow in a straight artery and confirm that the constraints placed upon our aneurysm models are conducive for aneurysm growth and rupture by comparing flow velocity in a straight artery and aneurysm with conditions simulated in past studies [5, 13]. We examine how

geometric factors of the splenic artery may contribute to the propensity for aneurysms to develop and rupture along the artery in §3.2 and show that dynamic pressure and wall shear stress values are higher in the artery with curved geometry than in the straight artery. Additionally, the range of dynamic pressure and wall shear stress is also greater in the curved artery. These results indicate that the curved geometry of the splenic artery predisposes it to promote aneurysm rupture and growth. In §3.3, we consider blood flow changes due to pregnancy or the addition of multiple aneurysms that may change hemodynamic variables underlying splenic artery aneurysm development and rupture. We show that velocity changes accompanying pregnancy exacerbate the aneurysm development conditions. In §4 we discuss the implications of our results and possible future studies.

2   Methodology

We discuss the mathematical model used to simulate blood flow variables in §2.1. We construct three dimensional geometries of a splenic artery and a straight artery with aneurysms in §2.2. We identify blood flow variables in §2.3 to compare between these geometries. We describe boundary conditions in §2.4.

2.1   Model

The Navier-Stokes equation (Equation 1), also called the vector momentum equation, describes three dimensional fluid flow where $\vec{u}$ is flow velocity of the fluid in a three dimensional field space that describes velocity in the x, y, and z directions.

$$\rho \frac{D\vec{u}}{Dt} = -\nabla p + \nabla \cdot \tau + \rho \vec{g} \tag{1}$$

$$\nabla \cdot \vec{u} = 0 \tag{2}$$

$$\tau = [\nabla(\mu(\vec{u})) + \nabla(\mu(\vec{u}))^T] \tag{3}$$

The left hand side of the Navier Stokes equation, $\rho \frac{D\vec{u}}{Dt}$, describes the rate of change of fluid particle momentum. Fluid density, ρ is set to $1050 kg/m^3$, consistent with values of blood density in [10]. Pressure is p, τ is the stress tensor, and $\vec{g}$ represents body acceleration. Blood is an incompressible fluid, meaning that its volume does not change depending upon the amount of pressure applied to it, which is incorporated in Equation 2.

Blood is a non-Newtonian fluid; its viscosity is not constant, but is dependent upon shear rate [14, 12]. Viscosity is constant in a Newtonian fluid and shear stress is linearly related to shear rate. The constant term describing velocity is the coefficient in the linear relationship between shear stress and shear rate. In non-Newtonian fluids shear rate and shear stress are non-linearly related, so viscosity must be defined as a function of shear rate instead of a constant. Blood, a pseudo-plastic fluid, is an amalgamation of various materials, including plasma and blood platelets [14].The Carreau model (Equation 4), simulates non-Newtonian fluids by relating viscosity, μ,and describing its changes, as a function of shear rate [14].

$$\mu_{eff}(\dot{\gamma}) = \mu_{\text{inf}} + (\mu_0 - \mu_{\text{inf}}) \left(1 + (\lambda\dot{\gamma})^2\right)^{\frac{n-1}{2}} \tag{4}$$

We set the material coefficients of the Carreau model using the variable values from [10]. The zero shear viscosity, $\mu_0 = 0.056$ (Pa*s) is the viscosity at zero shear rate. The infinite shear viscosity, $\mu_{\text{inf}} = 0.0035$ (Pa*s) is the viscosity at infinite shear rate. The relaxation time, $\lambda = 3.313$ (s), is the amount of time it takes for a viscous substance to

recover from shearing stress after flow has stopped [25], and the power law index is n= 0.3508. $\dot{\gamma}$ is shear rate. Shear rate describes the rate of change in velocity at which one layer of fluid passes over an adjacent lamina [26].

Critical hemodynamic variables that underlie aneurysm pathogenesis and rupture, such as wall shear stress, are dependent on viscosity [3, 22]. Fisher and Rossman examined wall shear stress distribution in Newtonian and non-Newtonian models and found that wall shear stress is more influential in non-Newtonian models than it is in Newtonian models [3]. Since we investigate aneurysm pathogenesis and rupture, it is critical to model underlying factors such as wall shear stress as accurately as possible through the Carreau model by accounting for changing viscosity. While there are advantages to modeling blood as Newtonian in certain models due to simplicity [13, 22, 5], for the purpose of this study, blood is modeled as a non-Newtonian fluid since aneurysm development variables, such as wall shear stress, may be more precisely modeled this way.

2.2   Geometries

We construct two three dimensional models of arteries in order to compare the splenic artery (Figure 2) to a straight artery (Figure 1). Figure 1 shows the shape of the straight artery that acts as the control. Figure 2 shows the curvy shape representing the splenic artery. We use a complex curve to closely mimic the natural shape of a splenic artery to yield more realistic results. The arteries have the same diameter.
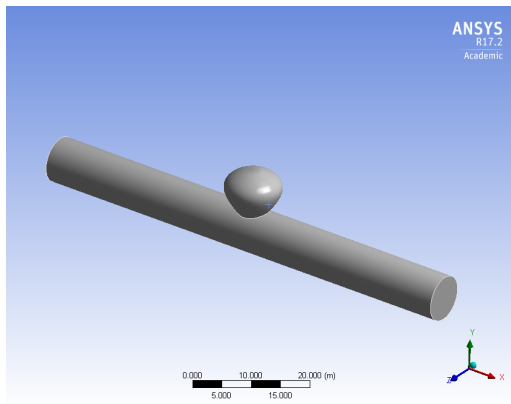

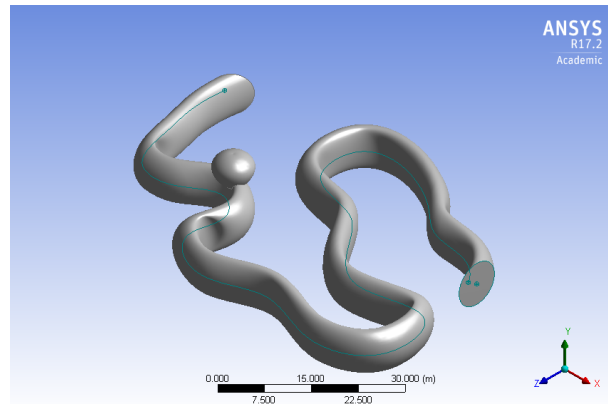Figure 1: Straight artery with aneurysm

Figure 2: Splenic artery with aneurysm

We place a single saccular aneurysm on each artery. A curve, created using the spline function in Ansys, is rotated 360 degrees around the vertical axis to form the aneurysm dome along the artery. Both arteries have the identical aneurysms, formed from the same spline function. The code used to generate the complex geometry of the splenic artery is provided as a supplemental file, which can be downloaded through the link provided. (https://www.dropbox.com/s/9um03komxzr9zbl/splenicCurvesketch%20%281%29.zip?dl=0). In the straight artery, the aneurysm is placed in the center of the artery length-wise. The aneurysm is placed on the distal end of the splenic artery, closer to the outlet. Past research has predicted aneurysm development location based on flow and pressure fields [5, 8], so the aneurysm was placed where the pressure values were highest in the geometry. The placement of the aneurysm is determined by examining locations of peak pressure values on a splenic artery model that did not contain an aneurysm.

The finite volume method is used for solving for these elements throughout these geometries using Ansys Fluent computational fluid dynamics solvers. Using these geometries, meshes are constructed using Ansys Meshing. There are 21806 elements in the straight artery mesh. There are 347807 elements in the splenic artery mesh. The straight artery is 90 cm and the splenic artery is approximately 210 cm. The diameters of both arteries are 8 cm.

Unlike compliant arteries, these models are rigid. However, previous research has found few significant differences in modeling flow simulations when comparing compliant to rigid vessels [20, 5]. The greatest limitation of these rigid boundaries is the inability for the aneurysm geometry to rupture. We seek to simulate hemodynamic conditions

that suggest impending rupture since the geometry does not alter. We can use rigid arteries to model the system as previous studies have done that involve rigid artery geometries in CFD simulations [20, 19, 8].

The algorithm in Ansys used to solve for the system is the SIMPLE algorithm. The SIMPLE algorithm is a velocity-pressure coupling algorithm that enforces mass conservation and obtains a pressure field from the coupled velocity and pressure. Time step size is 0.0025s. A minimum of 200 time steps was taken for each model. The maximum number of iterations per timestep is 200. If the convergence criterion has not been met after 200 iterations for a specific timestep, then the solver will stop the run for that timestep. The convergence criteria require that the scaled residuals decrease to 10^{-3} for all equations.

2.3 Blood Flow Factors

Previous studies have identified mechanisms underlying aneurysm formation in various arteries, including cerebral arteries [5, 22, 1, 13]. Hassani and Abdi concluded that blood pressure increases as expansion rate of the aneurysm increases [1]. Expansion rate rather than size of the aneurysm may be a better predictor of an impending aneurysm rupture [22]. Predicting when an aneurysm may rupture based on size alone may not be an accurate measure, although surgery is recommended when SAAs are 2 cm or larger [7]. A better indicator of an impending aneurysm rupture is a rapid significant change in size of the aneurysm [22]. Additionally, dramatic growth and hemodynamic changes occur at the neck of saccular aneurysms rather than the dome of the aneurysms [5]. The rigidity of the model will not allow us to model the changing size of the aneurysm but the accurate hemodynamic patterns and values obtained from the simulations of this model may indicate that in a flexible model, or blood vessel, the aneurysm will increase in size. We are interested in examining differences in blood flow factors between these artery geometries, since these factors indicate potential aneurysm growth and development.

Blood flow factors such as high wall shear rate and wall shear stress have been shown to be conducive for aneurysm pathogenesis and rupture [22, 13, 15, 5]. Wall shear stress increases velocity-pressure gradients [5] which cause aneurysm growth and formation [22]. High pressure and wall shear rates at the distal neck of the aneurysm cause aneurysm dilation [5]. Pressure in the vicinity of the aneurysm may grow to be over twice as high as the pressure of the parent artery [5].

We focus on the blood flow factors of dynamic pressure and wall shear stress since those variables have been shown to be critical in aneurysm pathogenesis and rupture [22, 13, 5, 1].

2.4 Boundary Conditions

We discuss the conditions placed at the inlet (§2.4.1), walls (§2.4.2) and the outlet (§2.4.3).

2.4.1 Inlet Velocity Conditions

We set the velocity as an inlet boundary as done in [13, 10]. Velocity in this model is non-constant and dependent on time since blood flow is pulsatile, changing periodically through the cardiac cycle as the heart chambers relax in diastole and contract in systole [14]. We define a velocity profile (Figure 3) to describe these periodic changes in velocity over time [10]. Blood flow velocity in an artery ranges from 0.1 m/s to 0.5 m/s for a healthy individual during one cardiac cycle (Figure 3).
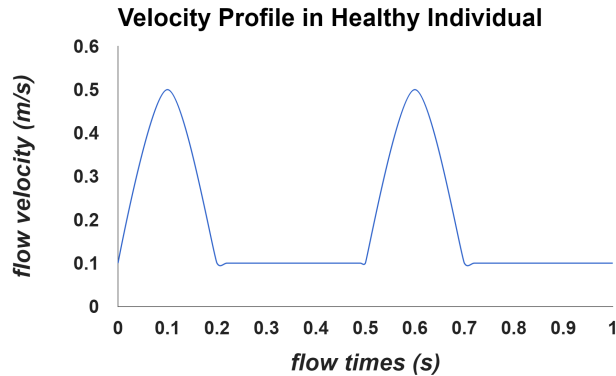
Velocity Profile in Healthy Individual

Figure 3: Pulsatile velocity profile as inlet condition in arteries modeled on non-pregnant individuals during a single cardiac cycle

2.4.2   No Slip Boundary Conditions

We assume no slip along the wall, $\vec{u}_{\text{wall}}$ = 0.

2.4.3   Pressure Conditions

We define pressure at the outlet to be 13332 Pa since we are modeling arteries in a closed system, rather than an open and exposed artery. Zero pressure outlets are often used as boundary conditions since they simplify models [5]. However, in some cases, the zero pressure outlet assumption can lead to an oversimplification of the model and misinformed conclusions [14]. Moon et al. [14] conclude that a zero pressure outlet simulates a blood vessel whose end is directly exposed to atmospheric conditions. A zero pressure boundary condition represents an open end of an artery, rather than a portion of a continuous closed artery, which is the artery represented in our research. Since the arteries simulated in this research are closed, the outlet pressure is set to 13332 Pa (100 mm Hg), the average of systolic, 15998 Pa (120 mm Hg), and diastolic pressure, 10665 Pa (80 mm Hg) in a healthy individual [10, 24]. This outlet pressure value is consistent with the boundary condition from previous research of similar closed models [10].

3   Results

We explore the straight artery and factors that influence its hemodynamics in §3.1. We compare in §3.2 hemodynamic variables in the straight artery and splenic artery. In §3.3 we model the hemodynamic changes that occur during pregnancy and when a second aneurysm forms along the artery to examine their influence on the splenic artery.

3.1   Straight Artery Modeling

Prior to comparing a straight artery with an aneurysm to a splenic artery with an aneurysm, we examine velocity flow in §3.1.1 in the straight artery to confirm that conditions in our model are conducive for aneurysm rupture. We examine wall shear stress in straight arteries in §3.1.2.

3.1.1   Velocity Vectors in Straight Arteries

We examine velocity vectors in the 3D straight artery at 60 sec (Figure 4) and in Animation 1 to confirm that fluid flow is consistent with previous research that identifies conditions for aneurysm growth and rupture [13, 5]. Animation 1

indicates the blood velocity in one second or one cardiac cycle throughout the artery. Fluid flow changes directions as it enters the aneurysm dome, forming a vortex which flows in a counter clockwise direction. This change in direction can be observed in the first five seconds of Animation 1. Additionally, we observe slower velocity within the higher portions of the dome, consistent with [5]. We observe more velocity variability and higher values at the neck of the aneurysm, rather than the ceiling of the dome, which supports that aneurysms are more likely to rupture at the neck rather than the ceiling of the dome [5]. Velocity, $\vec{u}$ is lowest along the walls of the artery geometry and increases with increasing distance from the walls. The low velocity values along the arterial walls are due to no slip boundary conditions along the walls where $\vec{u}_{\text{wall}} = 0$.
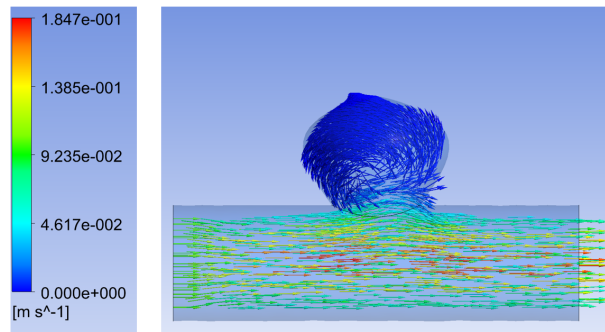

Figure 4: Velocity vectors in straight aneurysm at time t= 60 sec

3.1.2   Wall Shear Stress in Straight Arteries

We examine wall shear stress patterns in straight arteries at 1.1275 sec. Wall shear stress is not uniform throughout the straight artery (Figure 5). Similar to patterns in velocity, wall shear stress is lowest at the ceiling of the dome of the aneurysm in the straight artery.
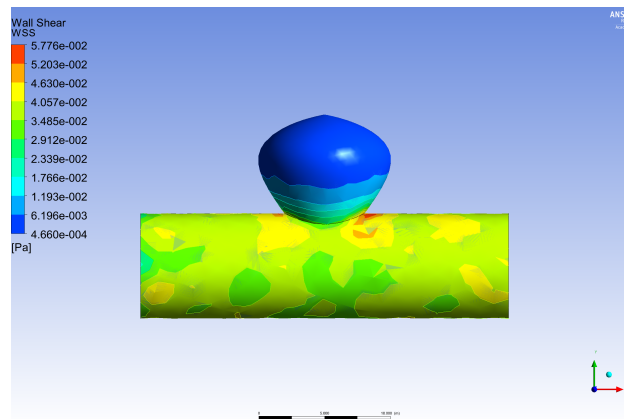

Figure 5: Wall shear stress is not uniform in straight artery aneurysm at t=1.1275 sec

3.2   Comparison of Straight Artery Aneurysm to Splenic Artery Aneurysm

We compare the straight artery geometry to the splenic artery. In §3.2.1 we compare dynamic pressure between the two geometries. In §3.2.2 we compare wall shear stress between the two artery geometries.

3.2.1 Dynamic Pressure Comparison

We compare dynamic pressure between the splenic artery and the straight artery at 1.135 sec. Dynamic Pressure, p reaches much higher values in the splenic artery of approximately 120 Pa compared to 6 Pa in the straight artery. Additionally, the wider range in p values in the splenic artery (Figure 6 B) is conducive for aneurysm development [5]. Although Figure 6 A appears to have constant pressure taken at this time, the dynamic pressure is not constant. The variety in pressure is much smaller in the straight artery in comparison to the pressure range in the splenic, so it is not visible on the large range. This difference in pressure variability throughout the arteries exposes how much larger the variation of pressure throughout the splenic artery is compared to the straight artery. Changes in dynamic pressure in the splenic artery may be observed in Animation 4. Dynamic pressure throughout the artery increases as the inlet velocity increases and decreases as inlet velocity decreases during the cardiac cycle (Figure 3), similarly to the changes in dynamic pressure observed in Animations 2 and 3 corresponding to changes in velocity in the inlet velocity profile (Figure 3). An animation of dynamic pressure changes in the straight artery is not included since the animation would not show any observable changes in dynamic pressure due to the range of pressure values, similarly to how dynamic pressure appears to be constant in Figure 6 A.
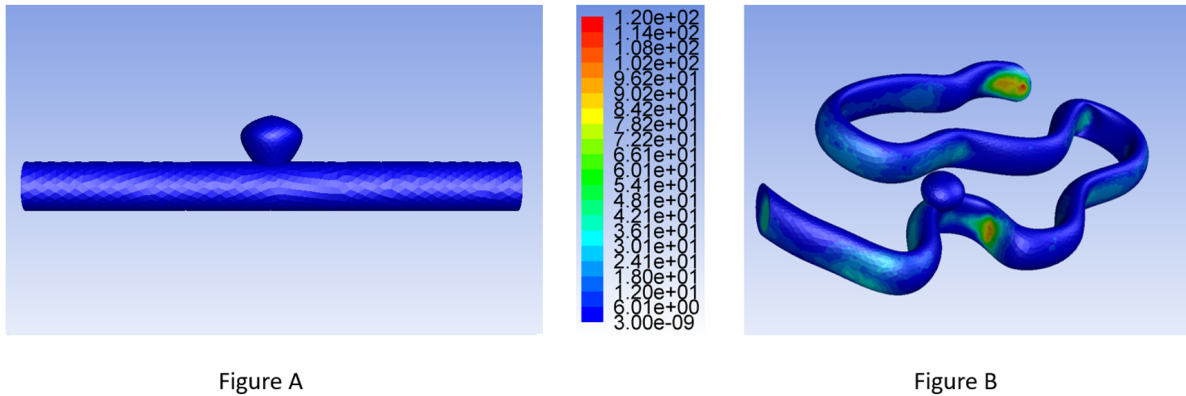

Figure A   Figure B

Figure 6: Dynamic Pressure of straight artery (A) and splenic artery (B) at t=1.135 sec

3.2.2 Wall Shear Stress Comparison

We compare values of wall shear stress between the straight artery and splenic artery at 1.1275 sec. These variables are compared when the splenic wall shear stress reaches a maximum value. Wall shear stress is much lower in the straight artery, ranging from $4.660 * 10^{-4}$ to $5.776 * 10^{-2}$ Pa (Figure 7 A) compared to $4.660 * 10^{-4}$ to 99.28 Pa (Figure 7 B) in the splenic artery. Changes in wall shear stress throughout the cardiac cycle in the splenic artery may be observed in Animation 5 and correspond to velocity changes in the inlet velocity profile. Wall shear stress throughout the artery increases as the inlet velocity increases and decreases as inlet velocity decreases during the cardiac cycle.
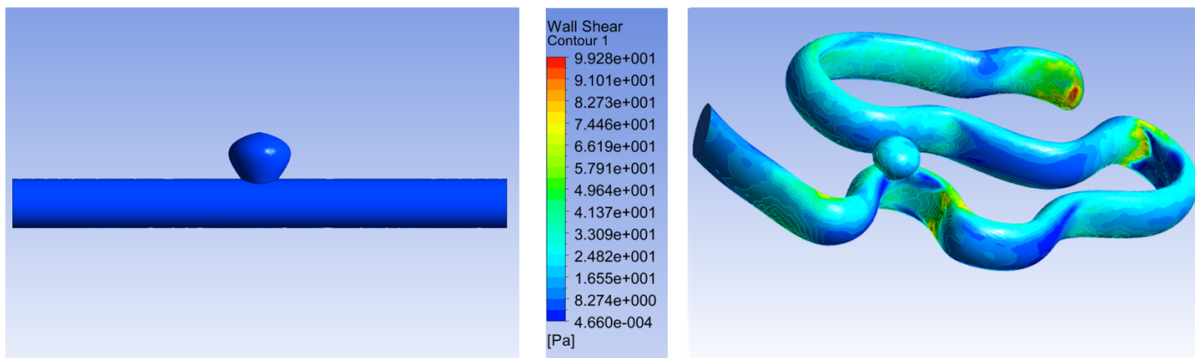
Figure A   Figure B

Figure 7: Wall shear stress in a straight artery (A) and a splenic artery (B) at t= 1.1275 sec

Similarly to the slight variation in dynamic pressure in the straight artery, wall shear stress does not have a constant value in Figure 7 A, the variation in wall shear stress in the straight artery in Figure 7 A is slight compared to the variation in the splenic artery in Figure 7 B. This difference in wall shear stress demonstrates how much larger the variation of wall shear stress in the splenic artery is compared to the straight artery. The wide range of wall shear stress values in Figure 7 B is too large for the variation in wall shear stress within the straight artery in Figure 7 A to be observable.

3.3   Splenic Artery Modeling

We compare various conditions occurring in the splenic artery with aneurysms. In §3.3.1 we compare how blood factors that change during pregnancy may affect splenic artery aneurysm development and rupture. In §3.3.2 we examine how multiple aneurysms along the splenic artery may affect aneurysm development and rupture.

3.3.1   Comparison of splenic artery under pregnancy conditions and non-pregnancy conditions

Pregnant women are more likely to develop splenic artery aneurysms than non-pregnant women [23, 18]. The physiological underpinning for this is not well understood. We create conditions in the splenic artery model to mimic the blood flow patterns within the artery of a pregnant woman to better understand how changes associated with pregnancy increase the risk of aneurysm development.

A significant change that occurs during pregnancy is an increase in peak velocity as a result of an increase in the amount of blood circulating throughout the body [21]. A cardiac cycle contains two peaks in velocity during diastole: E waves and A waves. E waves account for peak velocity during early diastole. In a non-pregnant individual, the average peak velocity for E is .857 m/s [4]. A waves occur after E waves, and typically have a lower peak velocity than E waves in healthy individuals. The average peak velocity of an A wave in a non-pregnant person is .558 m/s [4]. During pregnancy, these peak velocity values of A and E waves change. During the second trimester of pregnancy the E wave peak velocity significantly increases to 1.01 m/s and the A wave peak velocity increases to .64 m/s [4]. These two velocity profiles are described in Figure 8.

We modify the velocity profile to account for the variance between E waves and A waves during diastole in the cardiac cycle to model the peak velocity changes in pregnant women. We use the velocity profile described by [4] of healthy non-pregnant persons (red line) in Figure 8 to model the splenic artery of a non-pregnant woman. We use the velocity profile described by [4] of a healthy pregnant woman during the second trimester of pregnancy (blue line) in Figure 8 to model the splenic artery of a pregnant woman.

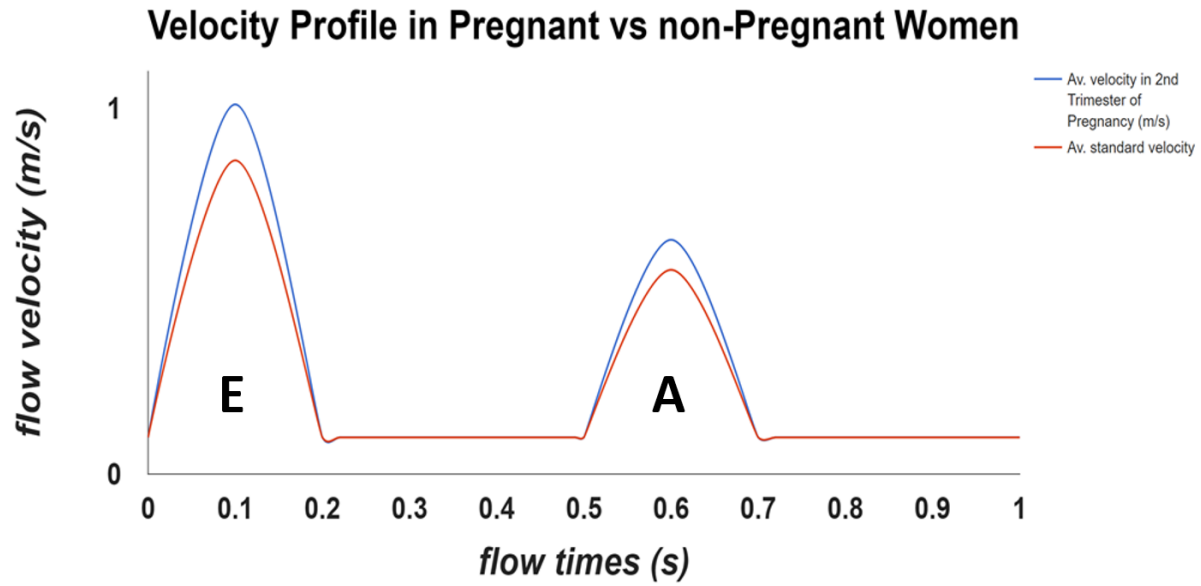**Velocity Profile in Pregnant vs non-Pregnant Women**

Figure 8: Velocity profile in women during second trimester of pregnancy (blue) and non-pregnant women (red) vs flowtime (s). The first peak is the E wave in diastole and the second peak is an A wave in diastole

Figure 9 shows the dynamic pressure at 0.055 sec in the cardiac cycle in splenic arteries of a pregnant and non-pregnant woman. The splenic artery of Figure 9 A models blood flow in the splenic artery of a women in her second trimester of pregnancy. Figure 9 B models blood flow in a splenic artery in a non-pregnant healthy woman.

The models indicate that an increase in peak velocity, associated with pregnancy, causes a significant increase in dynamic pressure throughout the splenic artery in pregnant women during the second trimester compared to the dynamic pressure in the splenic artery of a non-pregnant woman. This increase in dynamic pressure is associated with a higher risk for aneurysm development or rupture in the splenic artery [22, 13, 5, 1]. The results from our model indicate that the artery placed under conditions associated with pregnancy is at an increased risk for aneurysm development and is consistent with the clinical data that pregnant women are at an increased risk for developing aneurysms. These results show that pregnancy associated conditions, namely increased peak velocities, exacerbate the hemodynamic environment within the curved artery that is already prone to aneurysm development.

The dynamic pressure reaches a higher value of $1.38 * 10^4$ Pa in the splenic artery in Figure 9 A compared to the peak dynamic pressure of $1.105 * 10^4$ Pa in the splenic artery in Figure 9 B. In addition to the greater maximum pressure value, the range in dynamic pressure is also larger in Figure 9 A than it is in Figure 9 B. Both the range and higher peak velocity indicate that the splenic artery in a pregnant woman is at an increased risk for developing SAAs and having SAAs rupture along it.
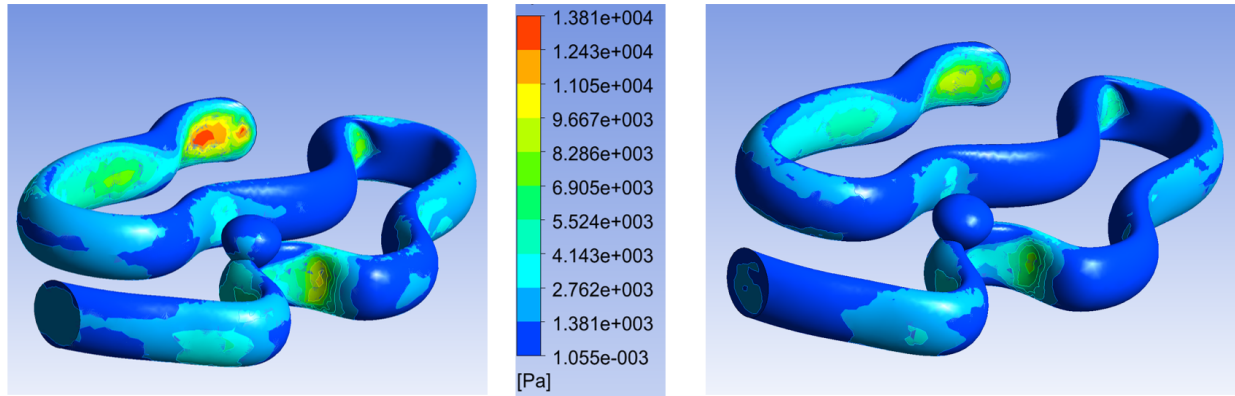
Figure A

Figure B

Figure 9: Dynamic pressure of splenic artery of a woman with an average velocity profile of the second trimester in pregnancy (A) and in splenic artery with typical peak velocity levels of non-pregnant women (B) at t= 0.055 sec

3.3.2 Comparison of splenic artery with multiple aneurysms

Typically, multiple splenic artery aneurysms develop on the artery rather than a single aneurysm developing [7]. We construct a second splenic artery containing two aneurysms (Figure 10 B). The second aneurysm is placed between the inlet and the first aneurysm, on the curve before the original aneurysm.

We use the same velocity profile of a non-pregnant woman in §3.3 (Figure 8 (red)), composed of the E and A waves as the inlet condition for the artery. We compare dynamic pressure in a splenic artery with a single aneurysm (Figure 10 A) and in a splenic artery with two aneurysms (Figure 10 B) under the same velocity inlet profile (Figure 8 (red)) at t= 0.055 sec.

Dynamic pressure is not largely influenced by the addition of a second aneurysm. Both the range and minimum and maximum values of dynamic pressure were the same in both arteries with a peak dynamic pressure of $1.016 * 10^4$ Pa and a minimum dynamic pressure of $4.965 * 10^{-2}$ Pa in both arteries (Figure 10 A and B). The similarities in dynamic pressure values and patterns in the two arteries indicate that multiple aneurysms do not significantly increase the risk of aneurysm rupture and growth compared to arteries with a single aneurysm.
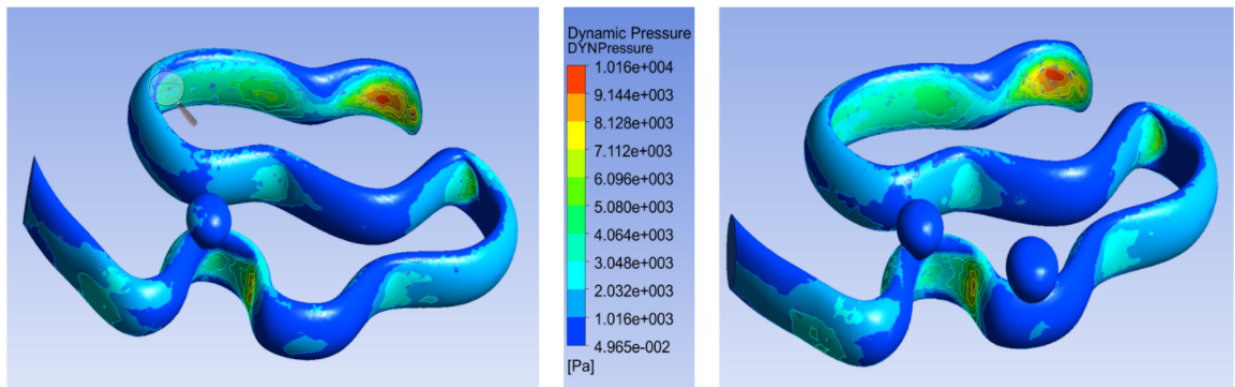

Figure A

Figure B

Figure 10: Dynamic pressure of splenic artery with a single aneurysm (A) and in splenic artery with two aneurysms (B) at t= 0.055 sec

4   Discussion

The large difference in hemodynamic variables such as dynamic pressure and wall shear stress between the straight artery and splenic artery under the same boundary conditions indicates that the geometry of the splenic artery uniquely predisposes it for aneurysm development. In comparison to straight arteries under the same conditions, the splenic artery reaches not only higher values of dynamic pressure, which are conducive for aneurysm growth and rupture, but also has a larger range of pressure, which exacerbates aneurysms [5].

Wall shear stress has similar results to dynamic pressure. Both the values and range of values for wall shear stress are greater in the splenic artery compared to those in the straight artery. Higher wall shear stress promotes aneurysm growth [5]. Wall shear stress is also higher on the aneurysm of the splenic artery compared to the aneurysm of the straight artery, supporting the theory that the splenic artery geometry promotes aneurysm growth and rupture.

Additionally, increased velocity values, which occur during pregnancy [4], increase dynamic pressure values that are conducive for aneurysm development and rupture. Women who have especially high blood velocity while pregnant may be at an increased risk for developing splenic artery aneurysms and SAA ruptures. Peak velocity is especially high during the second trimester, so it is likely that an SAA rupture would occur at that time during the pregnancy. Closely monitoring blood pressure throughout the pregnancy may better predict which women are at the greatest risk for developing splenic artery aneurysms and having SAAs rupturing. Taking these preventative measures may reduce maternal and fetal mortality rates resulting from ruptured SAAs.

However, adding a second aneurysm to the artery does not significantly affect the dynamic pressure in the splenic artery. The aneurysm addition suggests that compared to a single aneurysm along the artery, multiple aneurysms throughout the artery do not greatly impact the hemodynamic factors, such as dynamic pressure, of aneurysm development and rupture.

In the future, different aneurysm sizes may be considered. Comparing the numerical values of hemodynamic factors such as blood pressure and wall shear stress to clinical data may also be illuminating.

Finally, these geometries used to model aneurysms were rigid. Ruptures using this software would be impossible to model. In subsequent studies, modeling aneurysm development and rupture in flexible geometries and dynamic boundaries would provide more detailed results as to when a rupture would occur.

5   Acknowledgements

References

[1] M. ABDI, A. KARIMI, M. NAVIDBAKHSH, G. JAHROMI, K. HASSANI, A lumped parameter mathematical model to analyze the effects of tachycardia and bradycardia on the cardiovascular system, International Journal of Numerical Modeling, 23(2010), pp. 346âĂŞ357.

[2] J.R. CEBRAL, M.A. CASTRO, S. APPANABOYINA, ET AL., Efficient pipeline for image-based patient-specific analysis of cerebral aneurysm hemodynamics: technique and sensitivity. IEEE Trans Med Imaging 24(2005), pp. 457âĂŞ67.

[3] C. FISHER, J.S. ROSSMAN, Effect of non-newtonian behavior on hemodynamics of cerebral aneurysms, J Biomech Eng, 131(2009).

[4] W. Y. FOK, L. Y. CHAN, J. T. WONG, C. M. YU, T. K. LAU, Left ventricular diastolic function during normal pregnancy: assessment by spectral tissue doppler imaging, Ultrasound in Obstetrics % Gynecology, 28(2006), pp. 789-993.

[5] G. FOUTRAKIS, H. YONAS, R. SCHLABASSI, Saccular aneurysm formation in curved and bifurcating arteries, AJNR Am J Neuroradiol, 20(1999), pp. 1309-17.

[6] C.GONZALEZ, Y. CHO, H. ORTEGA, J. MORET, Intracranial Aneurysms: Flow Analysis of Their Origin and Progression, AJNR, 13(1992), pp. 181-188.

[7] A. T. GUILLAUMON, & E. A. CHAIM, Splenic artery aneurysm associated with anatomic variations in origin, J. Vasc. Bras., 8(2009), pp. 177-181.

[8] Y. HOI, H. MENG, S. H. WOODWARD, B.R. BENDOK, R. A. HANEL, L. R. GUTERMAN, L.N. HOPKINS, Effects of arterial geometry on aneurysm growth: three-dimensional computational fluid dynamics study, J. Neurosurgery, 101(2004), pp 676-681.

[9] W. JEONG, J. SEONG, Comparison of effects on technical variances of computational fluid dynamics (CFD) software based on finite element and finite volume methods, International Journal of Mechanical Sciences, 78(2014), pp. 19-26.

[10] C. JIANG, FLUENT Learning Modules: FLUENT - 3D Bifurcating Artery, Cornell University Confluence, Atlassian Confluence 5.8.18, 2014.

[11] L. KÃŞBORI, M. J. VAN DER KOLK, K. P. DE JONG, P. M. J. G. PEETERS, I. J. KLOMPMAKER, T. KOK, E. B. HAAGSMA, M. J. H. SLOOFF, Splenic artery aneurysms in liver transplant patients, Journal of Hepatology, 27(1997), pp. 890-893.

[12] B. LIU, J. ZHENG, R. BACH, D. TANG, Influence of model boundary conditions on blood flow patterns in a patient specific stenotic right coronary artery, Biomed Eng Online., 14(2015).

[13] D. A. LOTT, M. SIEGEL, H. R. CHAUDHY, C. J. PRESTIGIACOMO, Computational fluid dynamic simulation to assess flow characteristics of an in vitro aneurysm model, J NeuroIntervent Surgery, 2(2009) pp. 100-107.

[14] J. Y. MOON, D. C. SUH, Y. S. LEE, Y. W. KIM, J. S. LEE, Considerations of blood properties, outlet boundary conditions and energy loss approaches in computational fluid dynamics modeling, Neurointervention, 9(2014), pp. 1-8.

[15] T. G. PAPAIOANNOU, C. STEFANADIS, Vascular wall shear stress: basic principles and methods, Hellenic J Cardiology, 46(2005), pp. 9-15.

[16] S.F. PASHA, P. GLOVICZKI, A. W. STANSON, P. S. KAMATH, Splanchnic artery aneurysms, Mayo Clinic Proc., 82(2007), pp. 472-9.

[17] Y. PRIDE, B. RESTER, L. GARCIA, Splenic artery aneurysm: an endovascular approach to therapy, Vascular Disease Management, (2008).

[18] D. O. SELO-OJEME , C.C. WELCH, Review: spontaneous rupture of splenic artery aneurysm in pregnancy, Eur J Obstet Gynecol Reprod Biol., 109 (2003), pp. 124-7.

[19] S. S. SHISHIR, A K MIAH, S. ISLAM, T. HASAN, Blood Flow Dynamics in Cerebral Aneurysm - A CFD Simulation, Procedia Engineering, 105(2015), pp. 919-927.

[20] D. STEINMAN, J. MILNER. C. NORLEY, S. LOWNIE, D. HOLDSWORTH, Image-Based Computational Simulation of Flow Dynamics in a Giant Intracranial Aneurysm, AJNR, 24(2003), pp. 559-566.

[21] G. J. TSO, ET AL., Normal echocardiographic measurements in uncomplicated pregnancy, a single center experience, Journal of Cardiovascular Disease Research, 5(2014), pp. 3-8.

[22] A. VALENCIA, F. SOLIS, Blood flow dynamics and arterial wall interaction in a saccular aneurysm model of the basilar artery, Computers and Structures, 84(2006), pp. 1326-1337.

[23] A. ZUBAIDI, Rupture of multiple splenic artery aneurysms a common presentation of a rare disease with a review of literature, Saudi Journal of Gastroenterology Official Journal of the Saudi Gastroenterology Association, 15(2009), pp. 55âĂŞ58.

[24]   What is an Aneurysm?, American Heart Association, http://www.heart.org/HEARTORG/Conditions/VascularHealth/AorticAneurysm is-an-Aneurysm_UCM_454435_Article.jsp#.WPYGAdLyteU, 2016.

[25] Relaxation Time, Merriam Webster, https://www.merriamwebster.com/dictionary/relaxation%20time.

[26] Shear Rate, Schlumberger OilField Glossary, http://www.glossary.oilfield.slb.com/Terms/s/shear_rate.aspx.